Structure and magnetic properties of Cu-doped Sm Co 6.7 − x Cu x Cr 0.3 magnets

Q. Yao, W. Liu, X. G. Zhao, and Z. D. Zhang

Citation: Journal of Applied Physics **102**, 093905 (2007); doi: 10.1063/1.2802279
View online: http://dx.doi.org/10.1063/1.2802279
View Table of Contents: http://scitation.aip.org/content/aip/journal/jap/102/9?ver=pdfcov
Published by the AIP Publishing

Structure and magnetic properties of Cu-doped $SmCo_{6.7-x}Cu_xCr_{0.3}$ magnets

Q. Yao, W. Liu,[a] X. G. Zhao, and Z. D. Zhang
Shenyang National Laboratory for Materials Science, Institute of Metal Research, Chinese Academy of Sciences, Shenyang 110016, People's Republic of China and International Center for Materials Physic, Chinese Academy of Sciences, Shenyang 110016, People's Republic of China

(Received 3 April 2007; accepted 7 September 2007; published online 6 November 2007)

Structure and magnetic properties of mechanically alloyed Cu-doped $SmCo_{6.7-x}Cu_xCr_{0.3}$ ($x=0.1-0.7$) magnets have been systematically studied. The magnetically hard main phase is found to be of Th_2Ni_{17} type in the $SmCo_{6.7-x}Cu_xCr_{0.3}$ alloys. A small amount of Cu addition is favorable for the formation of the 2:17 phase/Co nanocomposite structure in the alloys. The increase of Cu doping results in more Cu precipitating in the alloys with separating the grains, which significantly enhances the intrinsic coercivity ${}_iH_c$ of the alloys and weakens the exchange coupling between the magnetically hard and soft phases. The magnetization reversal processes of the magnets have been discussed, upon the measurement of the recoil curves. © *2007 American Institute of Physics*. [DOI: 10.1063/1.2802279]

I. INTRODUCTION

Traditionally, it is well established that a high coercivity of sintered Sm_2Co_{17}-based magnets results from a cellular/lamellar precipitate microstructure with $Sm_2(Co,Fe)_{17}$ cells surrounded by the Cu-rich boundary phase, obtained by a multistage long duration thermal process.[1–4] This work has evolved from the initial work of Nesbitt *et al.*[5] with Cu serving as the principal element facilitating second-phase precipitation. Recently, these precipitation-hardened magnets have attracted considerable interest due to the need for developing magnets for high-temperature application. Near-zero or even large positive temperature coefficients of the intrinsic coercivity ${}_iH_c$ have been obtained in the precipitation-hardened $Sm(Co,Fe,Cu,Zr)_x$ series by arc melting[6,7] and rapid quenching[8,9] or in Zr-free Ti substituted $Sm(Co,Cu,Ti)_x$ magnets.[10] Since the intrinsic coercivity ${}_iH_c$ plays a crucial role in resisting the thermal demagnetization, increasing the intrinsic coercivity is a major objective to improve their high-temperature performance in the SmCo-based magnets with high Curie temperature. Mechanical alloying has been proved to be a powerful tool of synthesizing magnetic compounds such as $Nd_2Fe_{14}B$, $SmFe_7N_\delta$, and $Nd_2Fe_{14}C$,[11–14] and a high coercivity was obtained in Sm_xCo_{1-x} magnets by Ding *et al.*[15] using mechanical alloying and subsequent annealing. In our previous work, the coercivities of the mechanically alloyed (MA) $SmCo_{7-x}Cr_x$ magnets were significantly enhanced by increasing the Cr content.[16] In order to further enhance the intrinsic coercivity ${}_iH_c$ of the $Sm(Co,Cr)_7$ magnets, the addition of elemental Cu is expected to form the cellular microstructure in the $Sm(Co,Cu,Cr)_7$ magnets, similar to that in the $Sm(Co,Fe,Cu,Zr)_7$ magnets. In this article, effect of Cu addition on the structure and magnetic properties of MA $SmCo_{6.7-x}Cu_xCr_{0.3}$ ($x=0.1-0.7$) alloys is reported. In addition, the magnetization reversal process of the magnets is experimentally investigated.

II. EXPERIMENTAL DETAILS

Fine powders of elemental Sm, Co, Cu, and Cr with 99.5% purity with the compositions of $SmCo_{6.7-x}Cu_xCr_{0.3}$ ($x=0.1-0.7$) were milled for 5 h in a purified argon atmosphere in a high-energy ball mill rotated at a speed of 800 rpm in two dimensions perpendicular to horizontal plane.[12,13] The as-milled powders were annealed at 700 °C for 30 min in a vacuum better than 1.5×10^{-3} Pa. Powder x-ray diffraction (XRD) with Cu $K\alpha$ radiation was conducted to identify the phases in the samples. The major magnetic hysteresis loops at room temperature were measured using a pulsed magnetometer at fields up to 140 kOe. The demagnetization correction of the loops measured was performed by using an effective demagnetization factor of 0.28, experimentally determined. To understand the states of Cu and Co in the magnets, x-ray photoelectron spectroscopy (XPS) was performed with the Al $K\alpha$ line used as an x-ray source emitting at 1486.8 eV and with different etching times by argon ion sputtering. Demagnetization curves at temperatures ranging from 100 to 295 K and recoil curves at 295 K were measured by a superconducting quantum interference device (SQUID) at fields up to 70 kOe. The recoil curves were measured to analyze the reversal process of the magnets by applying a reverse field to the saturated sample in the remanent state and measuring the magnetic response upon reduction of the field to zero and back to the reversed field value. Each measurement along the recoil curves was preceded by a waiting time of 100 s to sufficiently avoid the magnetic viscosity effects. The amount of recoverable change in magnetization (M_{recov}/B_r) upon removal of the reversed field during recoil, as defined by Harland *et al.*,[17] was measured to investigate the interphase coupling of the magnets.

[a]Author to whom correspondence should be addressed. Electronic mail: wliu@imr.ac.cn

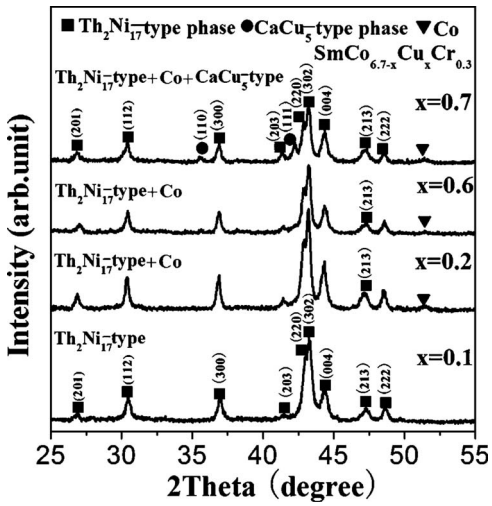

FIG. 1. XRD patterns of $SmCo_{6.7-x}Cu_xCr_{0.3}$ (x=0.1, 0.2, 0.6, and 0.7) alloys milled for 5 h and annealed at 700 °C for 30 min.

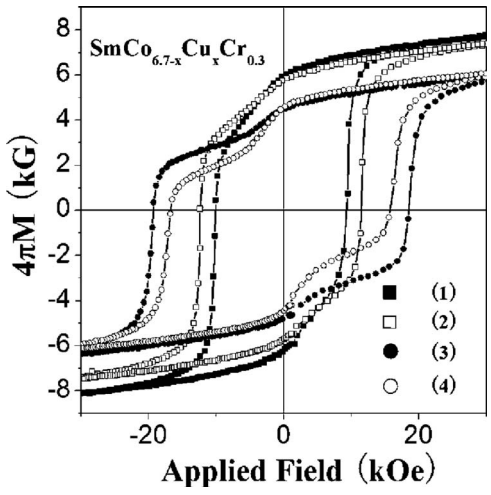

FIG. 2. Magnetic hysteresis loops at room temperature of $SmCo_{6.7-x}Cu_xCr_{0.3}$ (x=0.1, 0.2, 0.6, and 0.7) alloys milled for 5 h and annealed at 700 °C for 30 min: curves (1)–(4) are for x=0.1, 0.2, 0.6, and 0.7, respectively.

III. RESULTS AND DISCUSSION

Figure 1 represents the XRD patterns of $SmCo_{6.7-x}Cu_xCr_{0.3}$ (x=0.1, 0.2, 0.6, and 0.7) alloys milled for 5 h and annealed at 700 °C for 30 min. It is seen from Fig. 1 that the $Sm_2(Co,Cu,Cr)$ (Ref. 17) phase of Th_2Ni_{17} type appears as the main phase in the alloys over all the composition range, which were confirmed by the superlattice reflection peaks (213) and (203) (Refs. 16 and 18) also observed in the previous work.[16] A rather small peak around 2θ=51° is observed in the XRD pattern for $SmCo_{6.5}Cu_{0.2}Cr_{0.3}$, which maybe belongs to the reflection peak of Co with space group $Fm3m$. With increasing the Cu content x to 0.7, a small amount of $CaCu_5$-type $Sm(Co,Cu,Cr)_5$ phase coexists with the hexagonal 2:17 main phase in the alloy. The broadening of the peaks implies a fine grain size, which is in the range of 20–25 nm as estimated by the Scherrer formula.

The magnetic hysteresis loops at room temperature of $SmCo_{6.7-x}Cu_xCr_{0.3}$ (x=0.1, 0.2, 0.6, and 0.7) alloys milled for 5 h and annealed at 700 °C for 30 min are shown in Fig. 2. As also illustrated in Fig. 3(a), the intrinsic coercivity ${}_iH_c$ of the alloys increases significantly with increasing Cu content x from 9.5 kOe at x=0, reaches 19.4 kOe at x=0.6, and decreases to 16.8 kOe at x=0.7. Moreover, a slight step appears on the demagnetization curve of the $SmCo_{6.5}Cu_{0.2}Cr_{0.3}$ alloy. Further increasing the Cu concentration leads to the more pronounced steps on the demagnetization curves of the alloys, indicating the two individual reversal processes in the magnets. The remanent magnetization $4\pi M_r$ of the alloys decreases monotonously, as displayed in Fig. 3(b), from 8.7 kG at x=0 to 7.0 kG at x=0.7 with increasing the Cu addition.

The intrinsic coercivity characterizing the magnet hardness under the action of a reversed field can be affected by modifying either the magnetic anisotropy or microstructure of the materials. To clarify the factors causing the significant enhancement of the intrinsic coercivity ${}_iH_c$ in the $SmCo_{6.7-x}Cu_xCr_{0.3}$ alloys, the chemical states of Cu in the alloys were investigated by performing XPS. Figure 4(a) shows XPS survey patterns of the binding energy (BE) for Cu2p electrons with different etching times for the $SmCo_{6.1}Cu_{0.6}Cr_{0.3}$ alloy. It can be seen that Cu2p peaks on the powder surface are broad and low, which are quite different from the sharp and high Cu2p peaks with the etching time of 120–720 s. Moreover, the Cu2p peaks with the etching time of 0 s shift to the left when etched for 120–720 s. This suggests that the binding energy levels of Cu on the powder surface are higher than those inside. All these imply that Cu exists in the different states from the surface to the interior of the powders. To identify the chemical states of Cu in the alloy, the fitting curves of Cu2p3/2 with etching times of 0 and 120 s are shown in detail in Fig. 4(b). It is illustrated on the fitting curves that the Cu2p2/3 peak of 0 s etching time contains two BE states of 933.1 and 934.2 eV, corresponding to elemental Cu2p2/3 electrons[19] and CuO2p3/2 electrons,[20] respectively. The fitting curve of 120 s etching time, whose shape and position are the same with those of 420–720 s etching time, shows a single peak position of 933.1 eV. This means the existence of the elemental Cu inside the powders. The XPS results suggest that

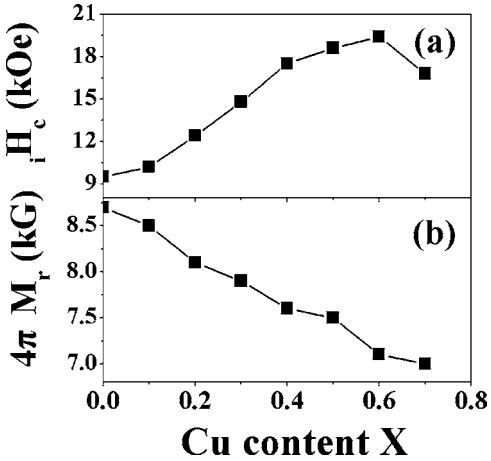

FIG. 3. Cu content dependence of (a) the intrinsic coercivity ${}_iH_c$ and (b) the remanent magnetization $4\pi M_r$ of $SmCo_{6.7-x}Cu_xCr_{0.3}$ (x=0–0.7) alloys milled for 5 h and annealed at 700 °C for 30 min.

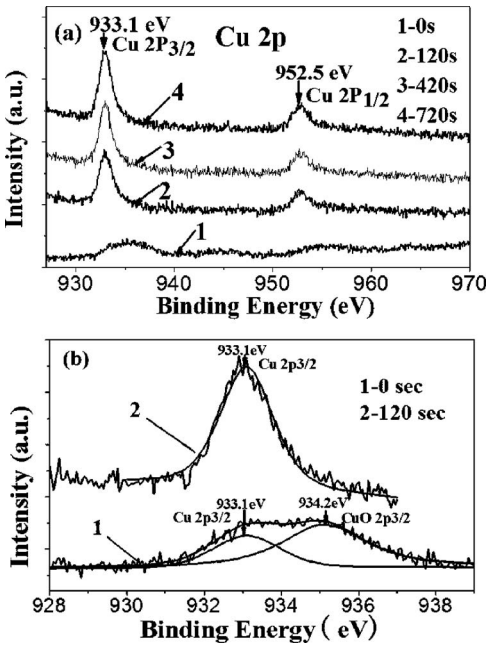

FIG. 4. (a) XPS survey patterns of the binding energy (BE) for Cu2*p* electrons with different etching times and (b) the fitting curves of Cu2*p*3/2 with etching times of 0 and 120 s for the $SmCo_{6.1}Cu_{0.6}Cr_{0.3}$ alloy.

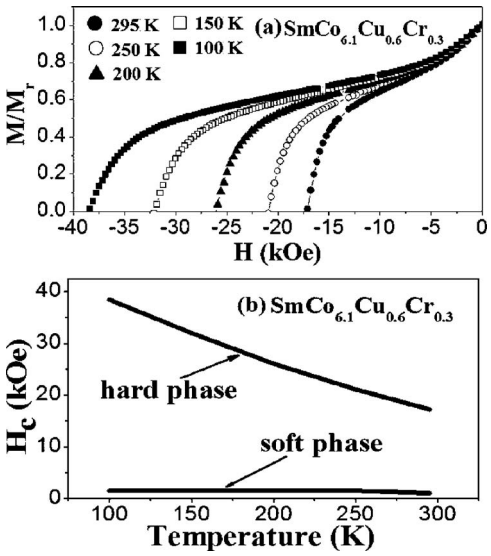

FIG. 5. Temperature dependence of (a) the demagnetization curves and (b) the coercive field H_c of the hard and soft phases for the $SmCo_{6.1}Cu_{0.6}Cr_{0.3}$ alloy.

Cu exists mainly in the form of elemental Cu in the powders, coexisting with CuO on the powders' surface. The precipitation of elemental Cu in the alloys, instead of the entry of Cu into the lattice of the 2:17 compound, may imply that Cu dopes at the edge of the crystalline grains or along the grain boundaries for its relatively low melting point (1083 °C). The elemental Cu precipitation may separate the grains from each other and greatly hinder the domain wall motivation, thus leading to the prominent enhancement of the intrinsic coercivity ${}_iH_c$ in the MA $SmCo_{6.7-x}Cu_xCr_{0.3}$ alloys. Similar phenomena have been observed in the melt-spun Pr–Fe–B ribbons with Cu addition.[21]

The two-step demagnetization behavior may result from the separate reversal processes of the different parts in the magnets, which is attributed to either the presence of magnetically hard and soft phases or the inhomogeneous ${}_iH_c$ distribution due to the coarse microstructure. Quantitative analyses of XPS results were made to show little variation of the at. % of Cu, for the samples scanned on the line and in the depth. It is suggested that Cu is distributed homogeneously in the alloys, without causing different resistance of domain wall motion leading to inhomogeneous magnetic hardness in the different parts of the magnets.

In order to investigate the factors causing the shoulders contained on the demagnetization curves of the $SmCo_{6.7-x}Cu_xCr_{0.3}$ alloys with $x=0.2-0.7$, demagnetization curves at temperatures ranging from 100 to 295 K for the $SmCo_{6.1}Cu_{0.6}Cr_{0.3}$ [shown in Fig. 5(a)] and $SmCo_{6.3}Cu_{0.4}Cr_{0.3}$ (not shown here) alloys were measured. It can be seen from Fig. 5(a) that the demagnetization curve contains a shoulder at 295 K, which becomes more pronounced with the decrease in the temperature. Similar observations were also found in melt-spinning $Pr_6Fe_{87}Nb_1B_6$ ribbons.[22] Moreover, it should be noticed that the intrinsic coercivity ${}_iH_c$ of the magnet significantly increases with decreasing the temperature while the step positions almost remain the same on the demagnetization curves. The increase of the intrinsic coercivity ${}_iH_c$ of the magnets can be ascribed to the enhancement of magnetic anisotropy of the hard 2:17 phase with reducing the temperature, similar to that observed in Sm–Fe–N magnets.[23] The temperature dependence of the intrinsic coercivity ${}_iH_c$ and the fields where the steps appear are plotted for the $SmCo_{6.1}Cu_{0.6}Cr_{0.3}$ [seen in Fig. 5(b)] and $SmCo_{6.3}Cu_{0.4}Cr_{0.3}$ (not shown here) alloys. As shown in Fig. 5(b) are the quite different trends for the intrinsic coercivity ${}_iH_c$ and the step positions with decreasing the temperature. The latter stays around 1.5 kOe, while the former varies distinctively and exhibits a significant increase as the temperature decreases. The intrinsic coercivity ${}_iH_c$ and the shoulders of the alloy denote the coercive fields H_c needed to reverse the hard and the soft components in the magnets, respectively. This has been confirmed by the calculated best-fit component magnetization curves of hard and soft characters for the Sm–Co/Fe bilayer film,[24] by using a simple model proposed by Stearns and Chen.[25] According to the micromagnetic theory[26,27] developed previously, the coercive field can be generally expressed as

$$H_c = \alpha_\varphi^{\text{eff}} \alpha_k \frac{2K_1}{\mu_0 M_s} - N_{\text{eff}} M_s,$$

where H_c, K_1, and M_s are the coercivity, the second-order anisotropy constant, and the saturation magnetization, respectively. $\alpha_\varphi^{\text{eff}}$ and α_k are microstructural coefficients related to the microstructure of the magnets. According to Kou *et al.*[28,29] $\alpha_\varphi^{\text{eff}}$ and α_k vary little in comparison with K_1 and M_s over wide temperature ranges. The temperature dependence of the coercive field H_c for each magnetic phase is mainly controlled by the temperature dependence of the intrinsic parameters K_1 and M_s of the magnetic phase. The totally different trends for the coercive field H_c of the hard and soft components with decreasing the temperature illus-

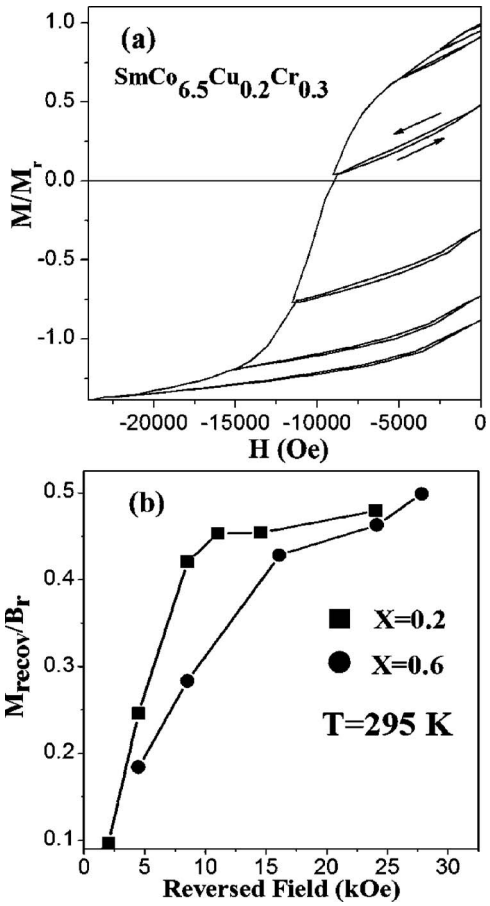

FIG. 6. (a) Normalized recoil curves for $SmCo_{6.5}Cu_{0.2}Cr_{0.3}$ alloys at 295 K. (b) Representative comparison of the normalized recovered magnetization M_{recov}/B_r at 295 K as a function of reversed field for $SmCo_{6.5}Cu_{0.2}Cr_{0.3}$ and $SmCo_{6.1}Cu_{0.6}Cr_{0.3}$ alloys.

trate the different K_1 and M_s of the two components, suggesting the presence of the hard and soft phases in the magnets. This is consistent with the XRD results (exhibited in Fig. 1) showing the appearance of a small amount of soft phase Co. Moreover, XPS results also confirm the existence of a small elemental Co separation except Co in the Sm_2Co_{17} compound states and in the Co_2O_3 oxidation states.

From the experimental observations, it is suggested that the MA $SmCo_{6.7-x}Cu_xCr_{0.3}$ alloys crystallize in the Th_2Ni_{17}-type 2:17 phase/Co nanocomposited structure with the elemental Cu precipitation. This structure is quite different from the cellular/lamellar microstructure in the sintered $Sm(Co,Fe,Cu,Zr)_x$ alloys with subsequent step aging.[1–4] Cu doping facilitates the partition of the soft Co phase with the hard Th_2Ni_{17}-type 2:17 phase and separates the grains from each other, thus weakening the coupling between the grains of the magnetically hard and soft phases. This may account for the shoulders contained on the demagnetization curves of the magnets.

In order to examine the magnetization reversal processes of the $SmCo_{6.7-x}Cu_xCr_{0.3}$ magnets with the Th_2Ni_{17}-type 2:17 phase/Co nanocomposited structure with the Cu addition, recoil curves were measured for the $SmCo_{6.7-x}Cu_xCr_{0.3}$ magnets at 295 K. Recoil curves measured from the major hysteresis loop back to zero internal field are shown in Fig. 6(a) for the $SmCo_{6.5}Cu_{0.2}Cr_{0.3}$ alloy. As illustrated in Fig. 6(a), recoil loops measured at reversed fields less than 2.2 kOe are almost completely reversible, tracing the major loop. Increasing the reversed fields above 2.5 kOe causes the recoil loops to deviate from the major demagnetization loop, indicating the occurrence of the irreversible reversal in this alloy. Application of reversed field greater than 5.0 kOe causes the recoil loops to open up (also observed by Goll *et al.*[30]), implying that a portion of the alloy is driven around a minor hysteresis loop. Harland *et al.*[17] reported the onset of recoil hysteresis signals of the soft phase decoupling from the hard phase and undergoing individual magnetic reversal. The recoil loops widen, with a maximum area obtained at reverse field of 11.4 kOe which is associated with the reversal of the hard phase of the magnet. Then the recoil loops become more and more closed as the reversed field increases. This is similar to the recoil hysteresis of Sm–Co/Fe bilayers observed by Kang *et al.*[24] Recoil hysteresis arising from the increasingly reversed fields represents an increased amount of phase reversal. Further increasing the reversed fields causes the reduced amount of reversing material participating in recoil, creating more closed recoil loops. Figure 6(b) exhibits the representative comparison of M_{recov}/B_r at 295 K as a function of reversed field for the $SmCo_{6.5}Cu_{0.2}Cr_{0.3}$ and $SmCo_{6.1}Cu_{0.6}Cr_{0.3}$ alloys, derived from the recoil loops of these alloys. It can be seen that a higher proportion of the available magnetization is recovered in the $SmCo_{6.5}Cu_{0.2}Cr_{0.3}$ magnet than in $SmCo_{6.1}Cu_{0.6}Cr_{0.3}$. It appears that the alloy with less Cu precipitation maintains a stronger exchange coupling between interphases, similar to that reported in Nd–Fe–B nanocomposite magnets by Harland *et al.*[17]

IV. SUMMARY

In summary, the hard Th_2Ni_{17}-type 2:17 phase is mainly formed in the MA $SmCo_{6.7-x}Cu_xCr_{0.3}$ alloys. Cu addition facilitates the separation of Co in the 2:17 phase matrix to form the 2:17 phase/Co nanocomposited structure in the magnets. Furthermore, elemental Cu precipitates as nonmagnetic substance in the magnetic powders and increases the resistance of the domain motion, thus significantly improving the intrinsic coercivities of the magnets. Increased Cu precipitation separates the grains from each other and weakens the exchange coupling between the grains, hence causing the appearance of steps on the demagnetization curves of the magnets. The recoil loop measurements show that the transition of reversible to irreversible reversal and the breakdown of the exchange coupling between the hard and soft phases are observed in the alloys with the hard 2:17 phase/Co nanocomposited microstructure.

ACKNOWLEDGMENTS

This work has been supported by the National Natural Science Foundation of China under Project Nos. 50331030, 50071062, and 59725103.

[1]G. C. Hadjipanayis, E. J. Yadlowsky, and S. H. Wollins, J. Appl. Phys. **53**, 2386 (1982).
[2]K. D. Durst, H. Kronmüller, and W. Ervens, Phys. Status Solidi A **108**,

403 (1988).
[3]A. E. Ray and S. Liu, J. Mater. Eng. Perform. **1**, 183 (1992).
[4]J. Strnat, IEEE Trans. Magn. **8**, 511 (1972).
[5]E. A. Nesbitt, R. H. Willens, R. C. Sherwood, E. Buehler, and J. H. Wernick, Appl. Phys. Lett. **12**, 361 (1968).
[6]J. F. Liu, T. Chui, D. Dimitrov, and G. C. Hadjipanayis, Appl. Phys. Lett. **73**, 3007 (1998).
[7]A. M. Gabay, W. Tang, Y. Zhang, and G. C. Hadjipanayis, Appl. Phys. Lett. **78**, 1595 (2001).
[8]D. Goll, I. Kleinschroth, W. Sigle, and H. Kronmüller, Appl. Phys. Lett. **76**, 1045 (1999).
[9]A. Yan, O. Gutfleisch, T. Gemming, and K.-H. Müller, Appl. Phys. Lett. **83**, 2208 (2003).
[10]J. Zhou, R. Skomski, C. Chen, G. C. Hadjipanayis, and D. J. Sellmyer, Appl. Phys. Lett. **77**, 1514 (2000).
[11]L. Schultz, J. Wecker, and E. Hellstern, J. Appl. Phys. **61**, 3583 (1987).
[12]W. Liu, Q. Wang, X. K. Sun, X. G. Zhao, T. Zhao, Z. D. Zhang, and Y. C. Chuang, J. Magn. Magn. Mater. **131**, 413 (1994).
[13]Y. C. Sui, Z. D. Zhang, Q. F. Xiao, W. Liu, X. G. Zhao, T. Zhao, and Y. C. Chuang, J. Phys.: Condens. Matter **8**, 11231 (1996).
[14]Z. D. Zhang, W. Liu, J. P. Liu, and D. J. Sellmyer, J. Phys. D **33**, R217 (2000).
[15]J. Ding, P. G. McCormick, and R. Street, J. Alloys Compd. **191**, 197 (1993).
[16]Q. Yao, W. Liu, X. G. Zhao, D. Li, and Z. D. Zhang, J. Appl. Phys. **99**, 053905 (2006).
[17]C. L. Harland, L. H. Lewis, Z. Chen, and B.-M. Ma, J. Magn. Magn. Mater. **271**, 53 (2004).
[18]M. Q. Huang, W. E. Wallace, M. McHenry, Q. Chen, and B. M. Ma, J. Appl. Phys. **83**, 6718 (1998).
[19]J. Haber, T. Machej, L. Ungier, and J. Ziokowski, J. Solid State Chem. **25**, 207 (1978).
[20]F. M. Capece, V. Dicastro, C. Furlani, G. Mattogno, C. Fragale, M. Gargano, and M. Rossi, J. Electron Spectrosc. Relat. Phenom. **27**, 119 (1972).
[21]Y. J. Zhang, L. Withanawasam, and G. C. Hadjipanayis, IEEE Trans. Magn. **28**, 2133 (1992).
[22]G. C. Hadjipanayis, J. Magn. Magn. Mater. **200**, 373 (1999).
[23]X. C. Kou, W. J. Qiang, H. Kromüller, and L. Schultz, J. Appl. Phys. **74**, 6791 (1993).
[24]K. Kang, L. H. Lewis, J. S. Jiang, and S. D. Bader, J. Appl. Phys. **98**, 113906 (2005).
[25]M. B. Stearns and Y. Chen, J. Appl. Phys. **75**, 6894 (1994).
[26]H. Kromüller, K. D. Durst, and G. Martinek, J. Magn. Magn. Mater. **60**, 149 (1987).
[27]H. Kromüller, K. D. Durst, and M. Sagawa, J. Magn. Magn. Mater. **74**, 291 (1987).
[28]X. C. Kou, E. H. C. P. Sinnecker, R. Grössinger, G. Wiesinger, W. Rodewald, and H. Kromüller, Phys. Rev. B **51**, 16025 (1995).
[29]X. C. Kou, H. Kromüller, D. Givord, and M. F. Rossignol, Phys. Rev. B **50**, 3849 (1994).
[30]D. Goll, M. Seeger, and H. Kromüller, J. Magn. Magn. Mater. **185**, 49 (1987).